Article ID:0253-2778(2016)04-0308-08

Threshold phenomenology of nucleon form factors

BALDINI FERROLI Rinaldo[1], PACETTI Simone[2], TOMASI-GUSTAFSSON Egle[3]

(1. *Laboratori Nazionali di Frascati dell'INFN, Frascati* 00044, *Italy*;
2. *Dipartimento di Fisica e Geologia e Sezione INFN, Perugia* 06123, *Italy*;
3. *CEA, IRFU, SPhN, Saclay, Gif-sur-Yvette Cedex* 91191, *France*)

Abstract: The complete knowledge of nucleon form factors is a mandatory pass to deeply understand the dynamics of strong interaction at regimes where QCD is still non perturbative. Phenomenology, i. e., the description of the data by means models based of first principles and depending on physical quantities, represents one of the most powerful tools to attain such a degree of knowledge.

Key words: Nucleon form factors; analyticity; threshold behavior; asymptotic behavior

CLC number: O572.3 **Document code**: A doi:10.3969/j.issn.0253-2778.2016.04.008

Citation: BALDINI FERROLI Rinaldo, PACETTI S, TOMASI-GUSTAFSSON E. Threshold phenomenology of nucleon form factors[J]. Journal of University of Science and Technology of China, 2016, 46(4): 308-315.

核子形状因子的阈值效应

BALDINI FERROLI Rinaldo[1], PACETTI Simone[2], TOMASI-GUSTAFSSON Egle[3]

(1. INFN 弗拉斯卡蒂国家实验室,弗拉斯卡蒂 00044,意大利;2. INFN 物理系,佩鲁贾 06123,意大利;
3. 法国原子能委员会萨克莱核研究中心,吉夫伊维特 91191,法国)

摘要:在微扰量子色动力学不再适用的低能区,核子形状因子可以作为一个重要参数来研究其强相互作用.诸如根据第一性原理和某个物理基本量的各种模型来描述数据的唯象物理学可以作为一个有效的工具来研究该领域.

关键词:核子形状因子;解析方法;阈值效应;渐进性

0 Definition and basic properties

0.1 Definitions

The nucleon form factors[1] (FFs) parametrize the factor to be associated to the photon-nucleon-antinucleon vertex, see Fig. 1, $\gamma N\overline{N}$, assuming extended nucleons, i. e., particles with non-pointlike charge and magnetic moment spatial distributions.

The Feynman amplitude of diagram in Fig. 1, in the space-like direction, i. e., for the scattering process, reads

$$\mathcal{M}=\frac{1}{q^2}e\bar{u}(k_2)\gamma_\mu u(k_1)e\overline{U}(p_1)\Gamma^\mu(p_1,p_2)U(p_2),$$

where e is the electron charge, u and U are the spinors of electrons and nucleons respectively, and

Received: 2015-11-30; **Revised**: 2016-04-20

Corresponding author: PACETTI Simone, PhD. Research field: high energy physics. E-mail: simone.pacetti@pg.infn.it

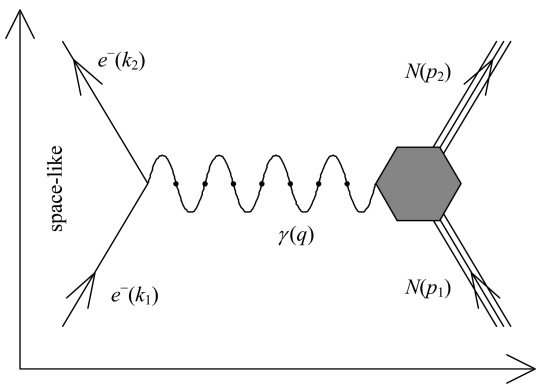

The hexagon represents the non-pointlike nucleon vertex.

Fig. 1 Feynman diagram of the one-photon exchange annihilation and scattering processes $e^+e^-\to N\overline{N}$ and $e^-N\to e^-N$

the four-momenta, in parentheses, are defined as in Fig. 1. The non-constant matrix, $\Gamma^\mu(p_1,p_2)$, which describes the nucleon vertex is

$$\Gamma^\mu(p_1,p_2)=\gamma^\mu F_1^N(q^2)+\frac{i\sigma^{\mu\nu}q_\nu}{2M_N}F_2^N(q^2) \quad (1)$$

where F_1^N and F_2^N are the Dirac and Pauli FFs. Such an expression represents the most general Lorentz four-vector, containing gamma matrices and nucleon four-momenta, that fulfills Lorentz, parity, time-reversal and gauge invariance. Form factors are scalar Lorentz functions of q^2, where q is the photon four-momentum.

0.2 Analyticity

The hexagon in Fig. 1 symbolizes the sum of all the electromagnetic contributions, i. e., all those diagrams having an arbitrary number of loops of all hadrons (computable in scalar quantum electrodynamics), with external lines only be photon, nucleon and antinucleon. The amplitudes of all these diagrams are analytic functions in the whole q^2 complex plane, except for a discontinuity cut, along the positive real axis, starting from $q_0^2=(2M_\pi)^2$. Such a threshold corresponds to the mass of the lightest hadronic state that can couple with the virtual photon. Moreover, the hermiticity of the electromagnetic current operator of the nucleons implies the Schwarz reflection principle for FFs so that, they are real for real q^2 outside the cut, while they have non vanishing imaginary parts for real $q^2>(2M_\pi)^2$.

0.3 Sachs form factors

From the expression of the nucleon electromagnetic four-current in terms of the Dirac and Pauli FFs,

$$J_N^\mu=e\overline{U}(p_1)\Gamma^\mu(p_1,p_2)U(p_2)=e\left(F_1^N+\frac{q^2}{4M_N^2}F_2^N,\overline{U}(p_1)\boldsymbol{\gamma}U(p_2)(F_1^N+F_2^N)\right),$$

another pair of FFs can be defined as

$$\left.\begin{aligned}G_E^N(q^2)&=F_1^N(q^2)+\tau F_2^N(q^2)\\G_M^N(q^2)&=F_1^N(q^2)+F_2^N(q^2)\\\tau&=\frac{q^2}{4M_N^2}\end{aligned}\right\} \quad (2)$$

These are the Sachs electric and magnetic FFs[2], that, in the Breit frame, where the nucleon four-momenta are $p_1=(E,-\boldsymbol{q}/2)$ and $p_2=(E,\boldsymbol{q}/2)$, represent the Fourier transforms of the nucleon charge and magnetization spatial distributions. It follows that their values at $q^2=0$ correspond to the total charge, Q_N, and magnetic moment, μ_N, of the nucleon, i. e., $G_E^N(0)=Q_N$, $G_M^N(0)=\mu_N$.

0.4 Measuring form factors

The differential cross section for the elastic scattering, in Born approximation, Feynman diagram of Fig. 1 in vertical direction, and in the laboratory frame (Lab), also known as Rosenbluth formula[3], reads

$$\frac{d\sigma_{eN}}{d\Omega}=\frac{\alpha^2\omega_2\cos^2\left(\frac{\theta_e}{2}\right)}{4\omega_1^3\sin^4\left(\frac{\theta_e}{2}\right)}\frac{1}{1-\tau}\cdot\left\{G_E^{N^2}(q^2)-\tau\left[1+2(1-\tau)\tan^2\left(\frac{\theta_e}{2}\right)\right]G_M^{N^2}(q^2)\right\} \quad (3)$$

while the annihilation cross section, in the same approximation, but in the e^+e^- center of mass frame (CoM), is[4]

$$\left.\begin{aligned}\frac{d\sigma_{N\overline{N}}}{d\Omega}&=\frac{\alpha^2\beta}{4q^2}\mathscr{C}\left[\frac{1}{\tau}\sin^2(\theta)\mid G_E^N(q^2)\mid^2+(1+\cos^2(\theta))\mid G_M^N(q^2)\mid^2\right]\\\beta&=\sqrt{1-\frac{1}{\tau}}\end{aligned}\right\} \quad (4)$$

where θ_e, $\omega_{1,2}$ are the scattering angle, the initial

and final energies of the electron in Lab, $\mathscr{C}$ is the Coulomb correction, θ is the scattering angle and β the velocity of the outgoing proton in CoM.

By studying the angular distributions of the scattering and annihilation processes, Sachs FFs can be measured: completely in the space-like region, $q^2<0$, where they are real; only in modulus in the time-like region, $q^2>0$, above the physical threshold $q_1^2=(2M_N)^2$, where they are complex. Moreover, by using only cross section data, the time-like complex structure of FFs remains inaccessible, as well as their values below the threshold q_1^2, in the so-called unphysical region, $0\leqslant q^2\leqslant q_1^2$.

Besides this procedure, FFs can also be measured by using polarization observables, i. e., by exploiting the so-called Akhiezer-Rekalo polarization method[5-6]. In particular, the polarization transferred to the nucleon, initially unpolarized, by longitudinally polarized electrons in a scattering process, allows to measure space-like FFs. More in detail, by exploiting of the scattering process $e^{-\uparrow}\ p\to e^-\ p^{\uparrow}$ (the up-arrow stands for polarization), the ratio between the transversal (in the scattering plane) and the longitudinal component of the outgoing proton polarization vector in Lab is proportional to the ratio of FFs[5-6], i. e.,

$$\frac{P_T^p(q^2)}{P_L^p(q^2)}=-\frac{2M_p\cot(\theta_e/2)}{\omega_1+\omega_2}\frac{G_E^p(q^2)}{G_M^p(q^2)},$$

where the symbols are those of Eq. (3).

In the annihilation process $e^+e^-\to N^{\uparrow}\overline{N}^{\uparrow}$, due to the complex nature of time-like FFs, unpolarized electrons produce polarized nucleons. In particular, the component, orthogonal to the scattering plane, of the nucleon polarization vector in CoM is[7]

$$P_{\perp}^N(q^2)=\frac{-\sqrt{\tau}\sin(2\theta)\left|\frac{G_E^N(q^2)}{G_M^N(q^2)}\right|}{\tau(1+\cos^2(\theta))+\sin^2(\theta)\left|\frac{G_E^N(q^2)}{G_M^N(q^2)}\right|^2}\sin(\Phi^N),$$

where symbols follow the labelling of Eq. (4) and Φ^N is the relative phase between electric and magnetic FFs. It follows that, by detecting the polarization of only one of the final nucleons, the phase of the complex ratio G_E^N/G_M^N can be measured.

0.5 Basic properties

The complex nature of the amplitude and hence of FFs, for time-like values of q, which is expressed formally by the optical theorem, lies in the fact that the photon, with such a four-momentum, gets enough virtual mass, $\sqrt{q^2}$, to couple with, and hence produce a series of on-shell hadronic intermediate states. Besides multi hadron ones, light vector meson resonances are the strongest coupled, i. e., the most probable intermediate states. They represent the main contributions to the FFs even though, having masses below the physical threshold $\sqrt{q_1^2}$, their peaks lie in the unphysical region. The complex structure of a prototype FF $F(q^2)$ is sketched in Fig. 2, where the three-dimensional surface (grid) represents the modulus squared $|F(q^2)|^2$ versus the unphysical q^2 complex plane. Indeed, it is in this Riemann sheet, where analyticity can be violated, that a generic resonance, of mass M_j and width Γ_j, manifests itself as a pair of complex conjugate poles z_j and $z_j{}^*$ (this is due to the Schwarz reflection principle), with① $z_j\backsimeq M_j^2+iM_j\Gamma_j$.

0.6 The asymptotic behavior

The space-like asymptotic behavior of FFs is inferred by means of dimensional counting rules of quantum chromodynamics[8-9]. At high space-like q^2, i. e. $q^2\ll-\Lambda_{\rm QCD}^2$, the momentum transferred by

① The position of the pole in the q^2 complex plane is strictly connected to the physical mass and width of the resonance, the definition of such quantities depends on the function used to describe the cross section. For instance, by using the relativistic Breit-Wigner formula and that in modulus squared reads $|BW(s)|^2=[(M_j^2-s)^2+\Gamma_j^2M_j^2]^{-1}$, the poles would be located exactly at $M_j^2\pm iM_j\Gamma_j$.

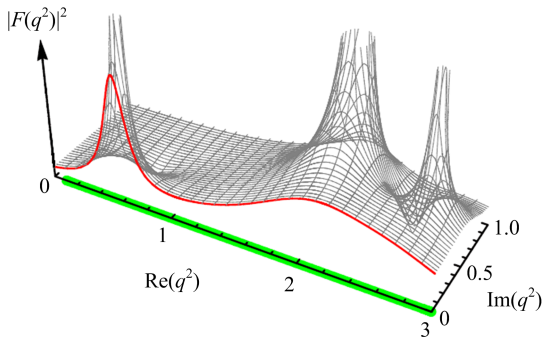

The grid surface represents the modulus squared of a prototype FF $F(q^2)$.
The poles are the resonances, the red curve is the $|F(q^2)|^2$ as it appears for real values of q^2, i. e. ,
it is the intersection between the surface and the plane $\mathrm{Im}(q^2)=0$.
The green band indicates the discontinuity cut $((2M_\pi)^2,\infty)$.

Fig. 2 Pictorial representation of first quarter of the q^2 unphysical complex plane

the virtual photon to the nucleon must be shared among the constituent quarks, in order for the nucleon to remain intact, by gluon exchanges.

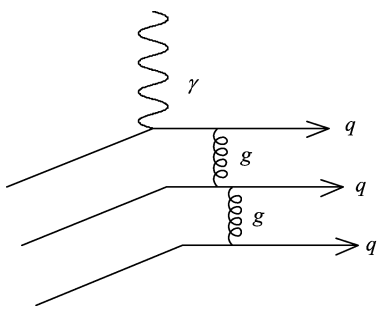

Fig. 3 Gluon (g) exchanges among the constituent quarks (q), to share the momentum transferred to the nucleon by the virtual photon

Following the schematic representation in Fig. 3, for the nucleons, that have three valence quarks, the minimum number of exchanges is two hence

$$F_i^N(q^2)\propto(-q^2)^{-1-i},\ q^2\to-\infty,$$

with $i=1,2$.

The Pauli FF has a further power $(-q^2)^{-1}$ since it is responsible for the spin-flip part of the nucleon electromagnetic current. The Sachs FFs, given in Eq. (2), have the same behavior

$$G_{E,M}^N(q^2)\propto(-q^2)^{-2},\ q^2\to-\infty.$$

The asymptotic behavior in the time-like region can be obtained by taking advantage from the analyticity and boundedness of FFs in the upper half plane, $\mathrm{Im}(q^2)>0$. Such regularities allow to apply the Phragmén-Lindelöf theorem[10] which ensures that FFs have the same vanishing power-law along any straight line from the origin to infinity, i. e. ,

$$\lim_{|q^2|\to\infty}\frac{G_{E,M}^N(|\ q^2\ |\ e^{i\pi})}{G_{E,M}^N(|\ q^2\ |\ e^{i\theta})}=1,\ \forall\,\theta\in[0,\pi].$$

The identity between space-like and time-like asymptotic behavior is verified by taking this limit with $\theta=0$. It follows that

$$G_{E,M}^N(q^2)\propto(q^2)^{-2},\ q^2\to\infty.$$

This result, since time-like FFs are complex, implies that imaginary parts vanish faster than the real ones

$$\lim_{q^2\to\infty}\frac{\mathrm{Im}[G_{E,M}^N(q^2)]}{\mathrm{Re}[G_{E,M}^N(q^2)]}=\lim_{q^2\to\infty}\arctan(\phi_{E,M}^N(q^2))=0,$$

i. e. , $\Phi_{E(M)}(q^2)$, the phase of the electric (magnetic) FF, tends to 2π radians as stated by the Levinson theorem[11].

1 The threshold

The threshold region is represented by few hundreds MeV, say δE, interval $(2M_N, 2M_N+\delta E)$, which starts at the time-like $N\overline{N}$ production energy. An e^+e^- collider operating at a CoM energy $E\in(2M_N, 2M_N+\delta E)$ would produce $N\overline{N}$ pairs almost at rest.

It is in this energy interval that charged nucleon and antinucleon experience the strongest electromagnetic interaction that, in the Born differential cross section formula of Eq. (4), is accounted for by the Coulomb factor $\mathscr{C}$. The expression of $\mathscr{C}$ can be obtained in the point-like limit as[12-13]

$$\mathscr{C}=|\ \psi_{\mathrm{Coul.}}(0)\ |^2=\frac{\pi\alpha}{\beta}\times\frac{1}{1-e^{-\pi\alpha/\beta}}\equiv\mathscr{E}\times\mathscr{R}\quad(5)$$

where $\psi_{\mathrm{Coul.}}(r)$ is the wave function solution of the Schrödinger equation with the Coulomb potential and β is the nucleon velocity given in Eq. (4). The two terms $\mathscr{E}$ and $\mathscr{R}$, called enhancement and resummation factor[14], account for the single and multi-photon contributions, respectively; $\mathscr{E}$

dominates at threshold where $\mathcal{R}\backsimeq 1$, i. e. ,

$$\mathcal{C}\backsimeq\mathcal{E}=\frac{\pi\alpha}{\beta},\ \beta\to 0^{+}.$$

The enhancement factor compensates for the closing of the phase-space by making the total Born cross section finite and different from zero at threshold, in particular[15]

$$\lim_{q^2\to 4M_N^2}\sigma_{N\bar{N}}(q^2)=\frac{\pi^3\alpha^2}{2M_N^2}\mid G^N(4M_N^2)\mid^2 \qquad (6)$$

where $G^N(4M_N^2)$ is the common threshold value of electric and magnetic FFs, that is, from the definitions of Eq. (2), assuming no singularities for the Dirac and Pauli FFs, $G_E^N(4M_N^2)=G_M^N(4M_N^2)\equiv G^N(4M_N^2)$. It follows that, the cross section and modulus of FFs can be measured even exactly at threshold. By taking advantage from the initial state radiation techniques, BaBar Collaboration measured $p\bar{p}$ cross section[16-17], practically reaching the threshold.

Solid and empty black circles in Fig. 4 represent two sets of BaBar data[16-17] on $e^+e^-\to p\bar{p}$ cross section, while the red point at the production threshold, which is indicated by the blue dashed line, is the expected value for the total cross section in case of

$$\mid G_E^p(4M_p^2)\mid=\mid G_M^p(4M_p^2)\mid=\mid G^p(4M_p^2)\mid=1.$$

In other words, assuming a flat cross section in the threshold region, BaBar Collaboration has measured, for the first time and at a percent level, a unit FF at threshold. Such a result seems to suggest that the physical threshold has a special meaning for the FFs, in contrast with their basic theoretical properties. Indeed, by considering an FF as the superposition of intermediate resonances and multi-hadron states, at these time-like four-momenta its value should be the sum of tails of these contributions, hence there is no reason for expecting this sum to be exactly one.

The flat $e^+e^-\to p\bar{p}$ cross section in the threshold region could be explained by considering:

① FFs almost constant and unitary;

② a resummation factor which accounts for multi-gluon exchanges ($\alpha\to\alpha_s$)

$$\mathcal{R}\to\mathcal{R}_s=\frac{1}{1-e^{-\pi\alpha_s/\beta}},\ \alpha_s=0.5.$$

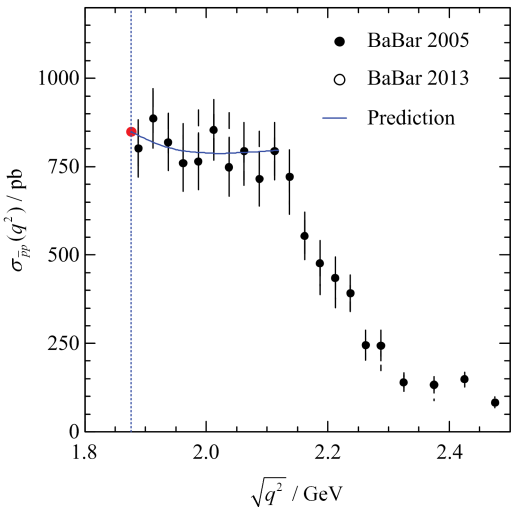

The blue dashed line indicates the physical threshold $\sqrt{q^2}=2M_p$. The solid red point at threshold represents the cross section expected if $|G_E^p(4M_p^2)|=|G_M^p(4M_p^2)|=|G^p(4M_p^2)|=1$. The blue curve is a prediction, see text.

Fig. 4 Total cross section of $e^+e^-\to p\bar{p}$, measured by the BaBar Collaboration in 2005, solid circles, and 2012, empty circles

In fact, in this case, the total cross section, that is obtained from the expression of Eq. (4) where all constants are reported in units of pb, becomes

$$\sigma_{p\bar{p}}(q^2)=[850\ \text{pb}]\frac{1}{\tau}\mathcal{R}_s,$$

and its behavior, shown as a blue curve in Fig. 4, describes the data quite well.

On the other hand, the effective FF

$$G_{\text{eff}}(q^2)=\sqrt{\frac{1}{\mathcal{R}}\frac{\sigma_{p\bar{p}}(q^2)}{\mathcal{E}\frac{4\pi\alpha^2}{3q^2}\beta\left(1+\frac{1}{2\tau}\right)}},$$

extracted from the BaBar cross section data, by considering the usual resummation factor (Eq. (5)) and as reported in Fig. 5, shows a steep decreasing behavior starting from the threshold that, having a flat cross section, turns out to be

$$G_{\text{eff}}(q^2)\backsimeq\frac{1}{\sqrt{\mathcal{R}}}=\sqrt{1-e^{-\pi\alpha/\beta}},$$

$$\sqrt{q^2}\in[2M_p,2M_p+\delta E].$$

The curve $1/\sqrt{\mathcal{R}}$ is shown in red in Fig. 5. It is

in perfect agreement with the BaBar data on $G_{\rm eff}(q^2)$, represented by black circles jointed by lines.

1.1 Isotropy at the $p\bar{p}$ production threshold

The identity of electric and magnetic FFs at the threshold is also interpreted as a consequence of isotropy.

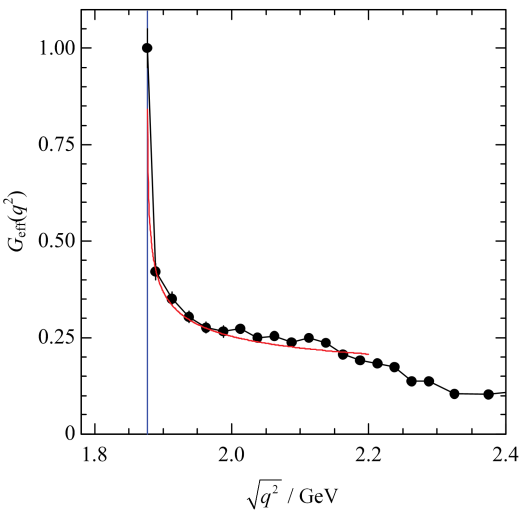

The red solid curve represents the function $1/\sqrt{\tau}$, see text.
The dashed blue line indicates the proton physical threshold.

Fig. 5 The black circles, but for the point at the threshold, which has been obtained by extrapolating the cross section, are the data on the effective proton FF measured by the BaBar Collaboration

Besides Sachs, Dirac and Pauli FFs, also partial wave FFs can be defined. From parity and total angular momentum conservation, in Born approximation, $N\overline{N}$ can be produced with only two values of orbital angular momentum, i. e., $L_{N\overline{N}}=0,1$. In fact, the $N\overline{N}$ system has to have parity $P_{N\overline{N}}=P_\gamma=-1$ and total angular momentum $J_{N\overline{N}}=J_\gamma=1$, where P_γ and J_γ are photon quantum numbers. Since, $P_{N\overline{N}}=(-1)^{L_{N\overline{N}}+1}$, -1 is the intrinsic $N\overline{N}$ parity, and the total spin is $S_{N\overline{N}}=0$, 1, it follows that: $L_{N\overline{N}}$ must be even ($L_{N\overline{N}}=0,2,\cdots$) and

$$J_{N\overline{N}}=1\in\{|L_{N\overline{N}}-S_{N\overline{N}}|,\cdots,|L_{N\overline{N}}+S_{N\overline{N}}|\},$$
$$=\begin{cases}\{1\} & (L_{N\overline{N}},S_{N\overline{N}})=(0,1)\\ \{1,2,3\} & (L_{N\overline{N}},S_{N\overline{N}})=(2,1)\end{cases},$$

all the other combinations $(L_{N\overline{N}},S_{N\overline{N}})$ give total angular momenta different from $J_\gamma=1$. Hence only S and D waves are allowed, the corresponding FFs are

$$G_S^N(q^2)=\frac{1}{3}(2\sqrt{\tau}G_M^N(q^2)+G_E^N(q^2)),$$
$$G_D^N(q^2)=\frac{1}{3}(\sqrt{\tau}G_M^N(q^2)-G_E^N(q^2)),$$

while the total annihilation cross section in CoM and in terms of G_S^N and G_D^N reads

$$\sigma_{N\overline{N}}(q^2)=\frac{2\pi\alpha^2\beta}{q^2}\frac{1}{\tau}[\mathscr{C}|G_S^N(q^2)|^2+2|G_D^N(q^2)|^2].$$

where the Coulomb correction acts only on the S-wave term. From the definitions of Eq. (7) follows that the isotropy at threshold, i. e., the presence at threshold of the only S wave and the vanishing of the D-wave contribution, is equivalent to the identity $G_E^N(q_1^2)=G_M^N(q_1^2)$.

Such an identity is experimentally observable, especially for lambda and sigma baryons, in a typical experiment at an e^+e^- collider (e. g. BESIII at BEPCII[18]). In particular, the ratio $|G_E^{\mathscr{B}}(q_1^2)/G_M^{\mathscr{B}}(q_1^2)|$ is measurable, even exactly at the production threshold. This is because all those $\mathscr{B}\overline{\mathscr{B}}$ final states where the (lambda or sigma) baryon, $\mathscr{B}$ (anti-baryon $\overline{\mathscr{B}}$), is at rest in the lab, can decay weakly into a nucleon (anti-nucleon) and a pion which have enough momentum to reach the detector.

Measuring a non-vanishing D-wave contribution, i. e., the inequality $|G_E^{\mathscr{B}}(q_1^2)/G_M^{\mathscr{B}}(q_1^2)|\neq 1$ would be the first observation of the analyticity-violation for the Dirac and Pauli FFs, that must have a simple pole at threshold ($\tau=1$) with opposite residues. In more detail, we define

$$F_1^{\mathscr{B}}(q^2)=\frac{-\Delta G^{\mathscr{B}}}{\tau-1}+F_{1,\rm an}^{\mathscr{B}}(q^2),$$
$$F_2^{\mathscr{B}}(q^2)=\frac{\Delta G^{\mathscr{B}}}{\tau-1}+F_{2,\rm an}^{\mathscr{B}}(q^2),$$

where $\Delta G^{\mathscr{B}}=G_E^{\mathscr{B}}(q_1^2)-G_M^{\mathscr{B}}(q_1^2)$ and $F_{1(2),\rm an}(q^2)$ is the analytic part of the Dirac (Pauli) FF. In this case, i. e., by allowing for different values of Sachs FFs at threshold and assuming $|\Delta G^{\mathscr{B}}|\ll|G_M^{\mathscr{B}}(q_1^2)|$, the annihilation differential cross section of Eq. (4) has the limit

$$\frac{{\rm d}\sigma_{\mathscr{B}\overline{\mathscr{B}}}}{{\rm d}\Omega}\xrightarrow[q^2\to q_1^2]{}$$

$$\frac{\alpha^2\beta}{3M_{\mathscr{B}}^2}[\,|\,G_M^{\mathscr{B}}(q_1^2)\,|^2+\mathrm{Re}(\Delta G^{\mathscr{B}}G_M^{\mathscr{B}^*}(q_1^2))\sin^2(\theta)].$$

It depends on the scattering angle, and hence is not isotropic, even at threshold. This can be also seen by considering the values of the partial wave FFs at $q^2=q_1^2$. They are

$$G_S^{\mathscr{B}}(q^2)\xrightarrow[q^2\to q_1^2]{}G_M^{\mathscr{B}}(q_1^2)+\frac{\Delta G^{\mathscr{B}}}{3}$$

$$G_D^{\mathscr{B}}(q^2)\xrightarrow[q^2\to q_1^2]{}-\frac{V\Delta G^{\mathscr{B}}}{3}.$$

As expected, the anisotropy, which is measured by the threshold value of $G_D^{\mathscr{B}}$, depends on difference between electric and magnetic FFs.

Unique sources of anisotropy are corrections due to $\mathscr{B}\overline{\mathscr{B}}$ final state interaction, that provide an overall power of β^{-2}, which means a simple pole for the FFs. Theoretical calculations give an order-α^2[19] effect in case of only Coulomb final state interaction (charged baryons). On the other hand strong Coulomb-like interaction, computed in case of heavy quarks[20], provides a large effect but is proportional to β^n ($n\in\mathbb{N}$), hence vanishing at threshold.

2 Conclusion

The threshold region for baryon FFs is a rich and unexplored mine of information on low-energy strong dynamics. Recently, in the $p\bar{p}$ final state, an FF oscillatory behavior has been clearly identified[21] and interpreted as a manifestation of $p\bar{p}$ final state interaction. Moreover, the observation of anisotropy, by measuring a value different from one for ratio between the moduli of Sachs FFs, is now suitable for experiments like BESIII[18]. Indeed, in such an experiment the detection efficiency for a $\mathscr{B}\overline{\mathscr{B}}$ pair of lambda or sigma baryons, is different from zero even exactly at threshold, when $\mathscr{B}\overline{\mathscr{B}}$ are produced at rest in Lab, since the decay products have always enough momentum to reach the detector.

From the theoretical point of view shedding light on the threshold behavior would help with understanding not only the nature of possible $\mathscr{B}\overline{\mathscr{B}}$ final state corrections still underestimated or neglected but also the unexpected unitary normalization observed in the case of $p\bar{p}$ and that seems to hold also for other $\mathscr{B}\overline{\mathscr{B}}$ channels[22].

References

[1] PACETTI S, BALDINI FERROLI R, TOMASI-GUSTAFSSON E. Proton electromagnetic form factors: Basic notions, present achievements and future perspectives[J]. Phys Rep, 2015, 550-551: 1-103.

[2] SACHS R G. High-energy behavior of nucleon electromagnetic form factors[J]. Phys Rev, 1962, 126: 2 256-2 260.

[3] ROSENBLUTH M N. High energy elastic scattering of electrons on protons[J]. Phys Rev, 1950, 79: 615-619.

[4] ZICHICHI A, BERMAN S, CABIBBO N, et al. Proton-antiproton annihilation into electrons, muons and vector bosons[J]. Nuovo Cim, 1962, 24: 170-180.

[5] AKHIEZER A, REKALO M. Polarization phenomena in electron scattering by protons in the high-energy region[J]. Sov Phys Dokl, 1968, 13: 572.

[6] AKHIEZER A, REKALO M. Polarization effects in the scattering of leptons by hadrons[J]. Sov J Part Nucl, 1974, 4: 277-278.

[7] DUBNIČKOVÁ A Z, DUBNIČKA S, REKALO M P. Investigation of the baryon electromagnetic structure by polarization effects in $e^+e^-\to B\overline{B}$ processes[J]. Nuovo Cim A, 1996, 109: 241-256.

[8] MATVEEV V, MURADYAN R, TAVKHELIDZE A. Scaling in strong interactions[J]. Teoret Mat Fiz, 1973, 15: 332-329.

[9] BRODSKY S J, FARRAR G R. Scaling laws at large transverse momentum[J]. Phys Rev Lett, 1973, 31: 1 153-1 156.

[10] TITCHMARSH E. The Theory of Functions[M]. Oxford: Oxford University Press, 1939.

[11] LEVINSON N. On the uniqueness of the potential in a Schrodinger equation for a given asymptotic phase[J]. Danske Vid Selsk Mat Fys Medd, 1949, 25(9): 1-29.

[12] SAKHAROV A D. Interaction of the electron and the positron in pair production[J]. Zh Eksp Teor Fiz, 1948, 18: 631-635.

[13] SOMMERFELD A. Atombau und Spektralliniem[M]. Braun-schweig, Germany: Vieweg, 1944, 2: 130.

[14] BALDINI FERROLI R, PACETTI S, ZALLO A. No Sommerfeld resummation factor in $e^+e^-\to p\bar{p}$? [J]. Eur Phys J A, 2012, 48(3):33.

[15] BALDINI R, PACETTI S, ZALLO A, et al.

Unexpected features of $e^+e^- \to p\bar{p}$ and $e^+e^- \to \Lambda\bar{\Lambda}$ cross-sections near threshold[J]. Eur Phys J A, 2009, 39: 315-321.

[16] AUBERT B, BARATE R, BOUTIGNY D, et al. Study of $e^+e^- \to p\bar{p}$ using initial state radiation with BABAR[J]. Phys Rev D, 2006, 73: 012005;

[17] LEES J P, POIREAU V, TISSERAND V, et al. Study of $e^+e^- \to p\bar{p}$ via initial-state radiation at BABAR[J]. Phys Rev D 2013,87:092005.

[18] CHAO K, WANG Y. Physics at BES-III [J/OL]. Int J Mod Phys A, 2009, 24 (supp01) [2015-11-30]. http://www. worldscientific. com/toc/ijmpa/24/supp01.

[19] DMITRIEV V F, MILSTEIN A I. Final state Coulomb interaction and asymmetry of pair production close to threshold in e^+e^- annihilation[J]. Phys Lett B, 2013, 722: 83-85.

[20] BRODSKY S J, HOANG A H, KUHN J H, et al. Angular distributions of massive quarks and leptons close to threshold [J]. Phys Lett B, 1995, 359: 355-361.

[21] BIANCONI A, TOMASI-GUSTAFSSON E. Periodic interference structures in the timelike proton form factor[J]. Phys Rev Lett, 2015, 114: 232301.

[22] BALDINI FERROLI R, PACETTI S. Baryon form factors at threshold[J]. Nucl Phys B(Proc Suppl), 2012, 225-227: 211-215.

(上接第 285 页)

References

[1] ANASHIN VV, AULCHENKO V M, BALDIN E M, et al. Measurement of main parameters of the $\psi(2S)$ resonance[J]. Phys Lett B, 2012,711(3/4):280-291.

[2] ANASHIN V V, AULCHENKO V M, BALDIN E M, et al. Final analysis of KEDR data on J/ψ and $\psi(2S)$ masses[J]. Phys Lett B,2015, 749:50-56.

[3] KURAEV E A, FADIN V S. On radiative corrections to e^+e^- single photon annihilation at high energy[J]. Sov J Nucl Phys, 1985,41:466-472.

[4] ANASHIN VV, AULCHENKO V M, BALDIN E M, et al. Measurement of R_{uds} and R between 3.12 and 3.72 GeV at the KEDR detector[EB/OL]. (2015-11-23)[2015-11-30]. http://arxiv.org/abs/1510.02667.

[5] AZIMOV Y I, VAINSHTEM A I, LIPATOV L N, et al. Electromagnetic corrections to the production of narrow resonances in colliding e^+e^- beams[J]. JETP Lett,1975, 21: 172.

[6] OLIVE K A, AGASHE K, AMSLER C, et al. Review of particle physics [J]. Chin Phys C, 2014, 38(09): 090001.